Energy Reports 12 (2024) 6016–6022

Contents lists available at ScienceDirect

Energy Reports

journal homepage: www.elsevier.com/locate/egyr

Research paper

Enhanced fault distance estimation for robust protection in unbalanced active distribution networks

S. Velasco-Gómez *, S. Pérez-Londoño, J. Mora-Flórez

Programa de Ingeniería eléctrica, Universidad Tecnológica de Pereira, ZIP:660003 Campus La Julita, Pereira, Colombia

ARTICLE INFO

Keywords:
Distance-based protection
Fault location
Fault resistance
Unbalanced distribution lines

ABSTRACT

Active Distribution Networks (ADN) have evolved significantly by integrating renewable energy sources. While these advancements have ushered in a more sustainable and efficient power system, these have also introduced challenges for traditional protection strategies. Conventional methods, often reliant on overcurrent relays, can struggle to adapt to the complexities of active distribution networks, where fault scenarios are diverse and dynamic.

This paper identifies the limitations of conventional protection strategies and explores the redundancy concept applied to protection systems. To improve protection system reliability, an approach that overcomes these limitations using the advantages of distance protection is proposed here. The distance-based protection relay, traditionally employed in transmission networks, offers a promising redundancy solution for the challenges imposed by ADN.

Considering the previous exposure, this paper introduces an algorithm for fault resistance and distance estimation designed to optimise the operation of distance relays in active distribution networks. The approach achieves remarkable accuracy with consistently low estimation errors for fault resistance and distance, regardless of fault type or distance. The proposed distance-based protection method is poised to revolutionise fault analysis in ADN, ultimately leading to faster fault isolation and more reliable and improved grid resilience.

1. Introduction

1.1. Motivation

The electrical system has evolved substantially, driven by the need for sustainability and adaptability to include diverse renewable energy sources generically denoted as Distributed Energy Resources (DER). The current electrical grid integrates several technologies, including new-generation sources, storage batteries, switchable microgrids, and controllable loads, which allows users to participate actively. This evolution has given rise to active distribution networks (ADN), which present unique problems due to their characteristics, such as unbalanced and bidirectional power flow, among others (Hooshyar and Iravani, 2017; Tsimtsios et al., 2019b; Mishra et al., 2020). These challenges create a critical need to propose redundant protection strategies that consider the complexities of ADN to improve their resilience, reliability and safety while providing high-quality electrical service to all users (Tang et al., 2024). This paper analyses a distance-based relaying approach as a viable alternative for redundant protection of ADNs.

1.2. State of the art

In recent years, many authors have proposed solutions to ensure that the protection system operates effectively in ADNs (García-Ceballos et al., 2021; Zhang et al., 2022; Biller and Jaeger, 2022). However, most of these proposals focus on overcurrent relays, as in Assouak and Benabid (2023), while others consider communication systems, which increase the budget significantly, as in Tsimtsios et al. (2019a). In addition, any electrical protection system reliant on communication necessitates resilience, nearly constant availability, and tightly controlled latency (Gutierrez-Rojas et al., 2020).

The main challenges faced by the protection system in ADN are rooted in the accurate detection of different fault types and the coordination of protection schemes because of a dynamic topology (Uzair et al., 2023). This challenge is due to several reasons, including that fault currents from DERs based on rotating or synchronous generators are sufficiently high. In contrast, the contribution of fault current is minimal in the case of DERs integrated into converters (Converter Integrated DER - CIDER) (Uzair et al., 2023). Additionally, fault resistance (R_f) impacts the estimation of the impedance observed by the distance

* Corresponding author.
E-mail addresses: sary.m.gomez@utp.edu.co (S. Velasco-Gómez), saperez@utp.edu.co (S. Pérez-Londoño), jjmora@utp.edu.co (J. Mora-Flórez).

https://doi.org/10.1016/j.egyr.2024.11.076
Received 22 August 2024; Received in revised form 16 November 2024; Accepted 25 November 2024
Available online 3 December 2024

protection (21), leading to improper relay operation. Some solutions involve estimating the currents contributed by the CIDER and R_f, as presented in Ghorbani and Mehrjerdi (2023). Even considering the use of artificial intelligence and machine learning techniques can be applied in microgrid protection to improve fault detection, classification, and coordination, as in Uzair et al. (2019), where a combination of multi-agent systems and machine learning helps to detect faults in grid-connected and islanded modes, relay coordination and adaptive relaying.

In addition, some strategies based on distance relay consider the integration of DER, as in George et al. (2023), Chao et al. (2022), and the authors in Ghorbani and Mehrjerdi (2023) also propose compensation for the effect of fault resistance. However, the majority of proposals are oriented towards transmission lines. as these presented in Banaiemoqadam et al. (2020), Liang et al. (2020), Zhang et al. (2023), which have distinct characteristics and challenges compared to distribution lines in ADNs (Velasco-Gómez et al., 2021).

On the other hand, some strategies protect DER at the Point of Interconnection (POI), mainly when dealing with single-line-to-ground since it is difficult to detect, especially in the case of ungrounded microgrids at the utility side of the transformer. Therefore, the authors in Yin et al. (2022) propose using distance relays to enhance apparent impedance estimation by compensating residual voltage, improving fault detection and location accuracy, and timely fault isolation. Finally, the paper (Velasco-Gómez et al., 2023) presents a proposed method for protecting unbalanced active distribution networks using distance relaying, but the fault impedance or CIDER presence needs to be considered.

Table 1 compares several relevant references in the literature with the proposed approach made in this research. The aspects considered for comparison are: (i) the consideration of CIDER modelling (CIDER), (ii) the analysis of different fault resistances (R_f), (iii) the consideration of line unbalance (Unbalance), (iv) sensitivity tests considering faults along the line (Fault distance), (v) requirement of communication infrastructure (Communication), (vi) and finally, the last three columns are associated to the field of application in transmission, distribution or active distribution networks (ADN).

As a conclusion derived from previous analysis, most proposals deal with the fault resistance effect, very few consider the structural unbalance of the lines, and only a few integrate CIDER. Moreover, it is observed that most of these approaches are proposed to protect transmission networks. Hence, proposing a protection strategy that accounts for the attributes considered in Table 1 while being independent of communication infrastructure is desirable in today's distribution systems.

1.3. Contribution

This paper presents an algorithm for accurately estimating fault resistance and distance online, which will be integrated into a redundant protection system for ADNs. This algorithm holds potential for integration into distance relays and other analysis tools. The principal contributions of the paper are:

- Accurate fault resistance and fault distance estimation used for the online determination of the faulted zone of a distance relay.
- Reliable estimation of the CIDER and load current downstream of the fault location.
- High performance and low computing burden approach to the opportune tripping signal definition.
- An additional protection strategy aimed to improve the protection system redundancy and then its reliability.

Table 1
Comparison of several distance-based relay protection strategies.

Reference	Main issues					Applied to:		
	CIDER	R_f	Unbalance	Fault distance	Communication	Transmission	Distribution	ADN
Tsimtsios et al. (2019a)	–	√	–	–	√	–	√	√
Ghorbani and Mehrjerdi (2023)	√	√	–	√	–	√	–	–
Liang et al. (2020)	–	√	–	√	–	√	–	–
Yin et al. (2022)	–	√	–	–	–	–	–	√
Song et al. (2023)	√	√	–	√	–	√	–	–
Li et al. (2023)	√	√	–	–	–	√	–	–
Filomena et al. (2008)	–	√	√	√	–	√	–	–
Mishra et al. (2021)	√	√	–	–	–	–	–	√
Abdollahzadeh (2023)	–	√	–	√	–	√	–	–
Proposed	√	√	√	√	–	–	√	√

1.4. Structure of document

In this manuscript, section two focuses on the conceptual foundations of distance protection and the source model employed. In the third section, the distance estimation algorithm is explained. The results and analysis are shown in the fourth section. Finally, section five presents the conclusions.

2. Conceptual foundations

This section presents a comprehensive exploration of the theoretical concepts underpinning distance protection and the Converter-Integrated Distributed Energy Resources (CIDER) control used in the proposed algorithm.

2.1. Basis of distance protection

The primary function of protective relays in active distribution networks is to detect and send a trip signal to isolate faults occurring on the distribution lines. Commonly, these networks are protected using overcurrent relays, but these experience problems when CIDERS are considered, as presented in Tsimtsios et al. (2019b), Hooshyar and Iravani (2017). The previous situation forces us to improve such protection functions and to develop a redundant protection system. Redundancy refers to the intentional duplication of protection functions or algorithms to increase reliability and ensure continued operation in case of unexpected problems in some parts of the entire protection system. The distance relay is a suitable protection alternative, first due to the availability of current and potential transformers required for the directional overcurrent relays, which can be used in this case, and second, its extensive use to protect conventional transmission systems nowadays.

The distance relay continuously measures the line voltages and currents; using the phasors obtained from these measurements, it calculates the positive sequence impedance (Z_e^1) from the relay location and the fault as presented in (1) and (2) for single phase and phase faults, respectively. This relay is adjusted with a zone setting impedance (Z_{set}^1), which represents the expected impedance at a specific distance from the relay location. This setting is typically based on the length and per unit length impedance of the distribution line being protected.

$$Z_e^1 = \frac{U_A}{I_A + I_0\left(\frac{z_{0_L}}{z_{1_L}} - 1\right)} \tag{1}$$

$$Z_e^1 = \frac{U_B - U_C}{I_B - I_C} \tag{2}$$

z_{1_L} and z_{0_L} are the per unit positive and zero sequence line impedance. A, B and C identifies the faulted phases; U and I are relay three-phase voltage and current.

Distance relay compares the calculated impedance (Z_e^1) with the zone setting impedance (Z_{set}^1). An estimated value of Z_e^1 lower than Z_{set}^1 indicates that the impedance measured is lower than expected, suggesting the presence of a fault along the protected line. If the impedance comparison indicates a fault condition, the distance relay opens the corresponding power breaker, disconnecting the faulted line.

2.2. Converter-Integrated Distributed Energy Resources (CIDER)

The average voltage source converter model, governed by an $0dq$ frame strategy, operating in grid-following, is the basis to determine the CIDER behaviour (Bahrani, 2021). The CIDER control broad concepts are presented in the following subsection, while the realistic source used is described in García-Ceballos et al. (2021).

2.2.1. Voltage source converter control

CIDER operates using a voltage source converter (VSC) controlled through an $0dq$ frame scheme to operate in grid-following mode. The control system involves two main control loops, defined as the inner and outer.

The inner loop focuses on current control, determining voltage references for the AC side based on current references from the outer loop. This control loop ensures a seamless power flow. This loop is defined by Eqs. (3) and (4).

$$u_{d_{ref}} = u_d - \omega L i_q + \left(k_{P_1} + \frac{k_{I_1}}{s}\right)(i_{d_{ref}} - i_d) \tag{3}$$

$$u_{q_{ref}} = u_q + \omega L i_d + \left(k_{P_1} + \frac{k_{I_1}}{s}\right)(i_{q_{ref}} - i_q) \tag{4}$$

Where $u_{d_{ref}}$ and $u_{q_{ref}}$ are the voltage references for the CIDER, which are the inner loop output. u_d, u_q and i_d, i_q are the dq voltages and currents measured at the CIDER connection node, which come from the Park transformation of u_{abc} and i_{abc}. ω is the system frequency, and θ is the angle reference for the Park transformation. k_{P1} and k_{I1} are the proportional and integral gains. L is the filter inductance between the CIDER and the network. $i_{d_{ref}}$, $i_{q_{ref}}$ are the reference currents at the inner loop and are the outputs of the outer loop.

The outer loop, dedicated to power control, shapes the inner loop current references, aligning the power output with predefined references. It also manages bidirectional power flow and maintains stability. This outer loop is critical in achieving this, mainly when keeping u_q at zero, guaranteeing reliable power output. The outer loop provides the inner loop current reference using the power reference. This control loop is defined by Eqs. (5) and (6) for grid-following mode CIDERs.

$$i_{d_{ref}} = \frac{p_{ref}\ u_d + q_{ref}\ u_q}{u_d^2 + u_q^2} \tag{5}$$

$$i_{q_{ref}} = \frac{p_{ref}\ u_q - q_{ref}\ u_d}{u_d^2 + u_q^2} \tag{6}$$

Where $i_{d_{ref}}$, $i_{q_{ref}}$ are the dq references for the inner loop. p_{ref}, q_{ref} are the references of active and reactive power for the outer loop, respectively. u_d and u_q are measurements as in (3) and (4).

Finally, using VSC provides significant advantages in enhancing the system's stability, particularly during severe disturbances. The correlation between stability and the system's ability to maintain synchronisation, a key influence of primary control, underscores the effectiveness of VSCs in stabilising the network (García-Ceballos et al., 2023).

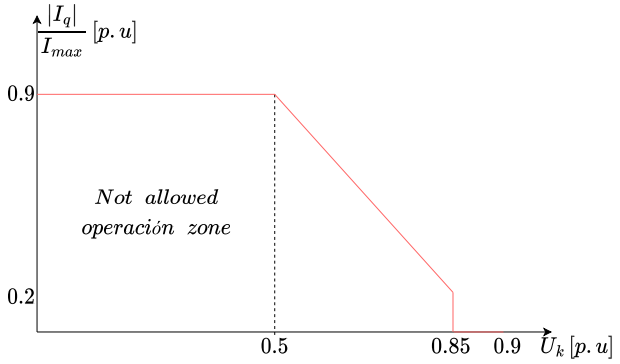

Fig. 1. Network code requirement for fault power factor.

2.2.2. Total current limiter

During abnormal conditions in the distribution network, such as faults, CIDER incorporates a critical safety mechanism to safeguard the converter. Eq. (7) comes into play, limiting direct axis current to protect against damage. This limiter ensures that CIDER remains operational despite network disturbances, delivering resilient power.

$$I_{d_{max}} = \sqrt{I_{max}^2 - I_q^2} \tag{7}$$

In Eq. (7), $I_{d_{max}}$ is a reference defined by the maximum permissible direct axis current; I_{max} is the highest current at the VSC that can be sustained without damage, even under fault conditions; I_q is the quadrature axis current measured at the PCC. Additionally, $|I_q| \leq |I_{max}|$.

The R/X ratio in low-voltage microgrids frequently reaches significant values. As a result, voltage support primarily relies on the direct axis current, I_d, while the reactive power linked to I_q predominantly influences the grid's frequency.

2.3. Reactive support requirement

The reactive support requirement is defined by the quadrature current fed by CIDER, which is necessary to enhance the network voltage profile after the fault's inception. The minimum required reactive support current, as presented in Fig. 1, is generally defined by national codes. The reference used in this paper is obtained from Hooshyar et al. (2014).

Finally, the CIDER control considered in this paper integrates the inner and outer loops and the requirements associated with the total current limiter and the reactive support requirement previously presented.

3. Approach for distance-based protection in unbalanced ADN

The proposed algorithm enhances the existing distance-based relays by enabling the accurate and fast determination of the fault resistance (R_f), fault distance (d), and CIDER remote current (I_g). The determined values are used to improve the conventional distance relays, thereby improving the accuracy of the protection system during fault conditions.

The developed algorithm is illustrated in Fig. 2, and the application for all shunt fault types (ground and phase faults) is outlined in the subsequent subsections.

3.1. Single-phase-to-ground fault case

This section is oriented to develop an accurate fault distance and resistance estimation algorithm considering single-phase faults. Distributed energy sources integrated using converters are considered and modelled for the proposed analysis. Fig. 3 shows a simplified distribution system representation and the used variables.

Each of the steps in the proposed algorithm is described below:

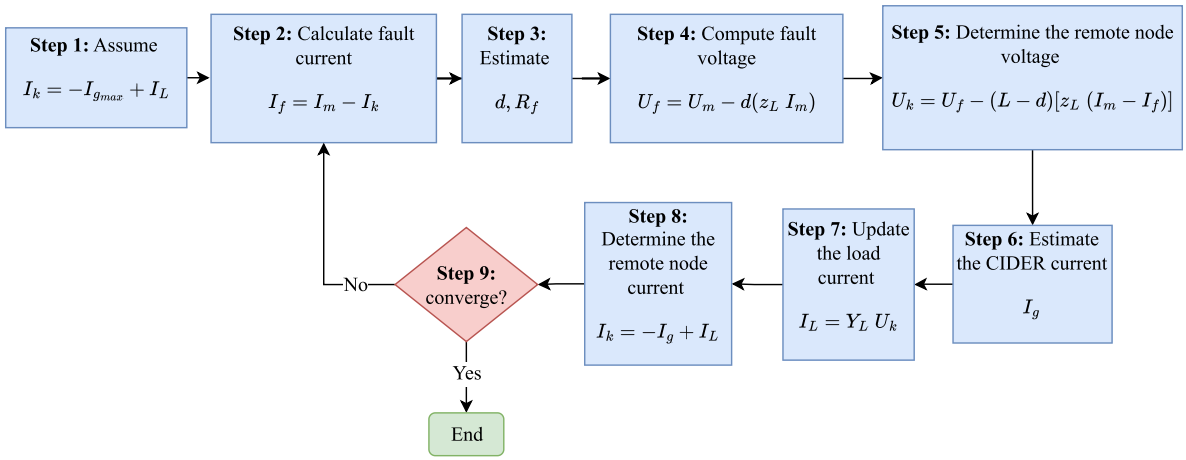

Fig. 2. Block diagram of the proposed algorithm.

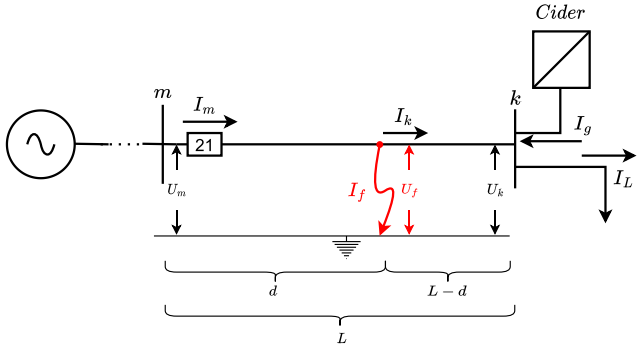

Fig. 3. Fault system representation.

3.1.1. Step 1: Assume the remote node current

The current phasor at node k, denoted as ($\boldsymbol{I}_k$), is assumed using pre-fault data as shown in Eq. (8)

$$\boldsymbol{I}_k = -\boldsymbol{I}_{g_{max}} + \boldsymbol{I}_L \tag{8}$$

3.1.2. Step 2: Calculate the fault current

The fault current phasor ($\boldsymbol{I}_f$), is computed using the measured current ($\boldsymbol{I}_m$), as presented in (9).

$$\boldsymbol{I}_f = \boldsymbol{I}_m - \boldsymbol{I}_k \tag{9}$$

3.1.3. Step 3: Estimate the fault distance

Eqs. (10) and (11) are used to determine the fault distance and resistance .

$$R_f = \frac{-C_2 U^x_{m_r} + C_1 U^x_{m_i}}{C_1 I^x_{f_i} - C_2 I^x_{f_r}} \tag{10}$$

$$d = \frac{I^x_{f_i} U^x_{m_r} - I^x_{fr} U^x_{m_i}}{C_1 I^x_{f_i} - C_2 I^x_{f_r}} \tag{11}$$

In the previous equations, the superscript x indicates the faulted phase and the subscript indices denote the real and imaginary components, respectively. C_1 and C_2 are defined as presented in (12) and (13).

$$C_1 = \sum_{n=a,b,c} [z_{an_r} I_{mn_r} - z_{an_i} I_{mn_i}] \tag{12}$$

$$C_2 = \sum_{n=a,b,c} [z_{an_r} I_{mn_i} + z_{an_i} I_{mn_r}] \tag{13}$$

Where, z_{an} is the line mutual impedance of phases a and n, $n = a, b, c$, and subscripts r and i denotes real and imaginary values.

3.1.4. Step 4: Estimate the voltage at the faulted node

Calculate the fault voltage phasor ($\boldsymbol{U}_f$) using the Eq. (14).

$$\boldsymbol{U}_f = \boldsymbol{U}_m - d(z_L\ \boldsymbol{I}_m) \tag{14}$$

3.1.5. Step 5: Estimate the voltage at the remote node

The voltage phasor at node k ($\boldsymbol{U}_k$), is estimated as indicated in Eq. (15).

$$\boldsymbol{U}_k = \boldsymbol{U}_f - (L-d)[z_L\ (\boldsymbol{I}_m - \boldsymbol{I}_f)] \tag{15}$$

3.1.6. Step 6: Determine the CIDER current

The current in the converter (I_g) is updated taking into account the source model. Relation among voltage and quadrature current is defined considering Fig. 1, and as presented in (16).

$$\frac{|I_q|}{I_{max}} \geq \begin{cases} 0.9 \quad \forall \quad U^x_k \leq 0.5 \\ \left(-\frac{18}{7} U^x_k + \frac{153}{70}\right) \quad \forall \quad 0.5 < U^x_k \leq 0.85 \\ 0 \quad \forall \quad 0.85 < U^x_k \end{cases} \tag{16}$$

Now, it calculates I_d, as explain in (7).

Then, I_g is calculated:

$$I_{g_{mag}} = \sqrt{I_q^2 - I_d^2}$$
$$I_{g_{ang}} = arctan(\frac{I_q}{I_d}) \tag{17}$$

Therefore,

$$I_g = I_{g_{mag}} cos(I_{g_{ang}}) + i\ I_{g_{mag}} sin(I_{g_{ang}}) \tag{18}$$

The converter currents are out of phase ($1\angle 120°$).

3.1.7. Step 7: Estimate the load current

The load current phasor ($\boldsymbol{I}_L$), in case of loads downstream the fault, is updated as shown in (19).

$$\boldsymbol{I}_L = \boldsymbol{Y}_L\ \boldsymbol{U}_k \tag{19}$$

Where $\boldsymbol{Y}_L$ represents the impedance load model, which is parameterised considering the pre-fault active and reactive power to include the normal hourly load size variation. This is usually defined as a voltage-dependent load model.

3.1.8. Step 8: Calculate the remote node current

Update the current phasor at node k ($\boldsymbol{I}_k$) as indicated in (20).

$$\boldsymbol{I}_k = -\boldsymbol{I}_g + \boldsymbol{I}_L \tag{20}$$

3.1.9. Step 9: Determine the convergence of the solution

Finally, convergence is analysed as (21).

$$R_f(i) - R_f(i-1) \leq \epsilon \tag{21}$$

Variable ϵ is defined as a precision requirement. If the convergence criterion is not satisfied, the fault current is updated as indicated in step 2 and continues with the following steps; otherwise, the algorithm is completed.

3.2. Phase fault case

The algorithm for fault distance estimation in the case of phase faults (double-phase, double-phase-to-ground and three-phase-to-ground faults) is similar to the previously presented. However, the estimation of R_f and d is determined as presented in Eqs. (22) and (23). The estimation is included in step 3 of the proposed algorithm.

$$R_f = \frac{-C_4(U_{mn_r} - U_{mx_r}) + C_3(U_{mn_i} - U_{mx_i})}{C_3 I_{f_i} - C_4 I_{f_r}} \tag{22}$$

$$d = \frac{I_{f_i}(U_{mn_r} - U_{mx_r}) - I_{fr}(U_{mn_i} - U_{mx_i})}{C_3 I_{f_i} - C_4 I_{f_r}} \tag{23}$$

Where, $n, x = a, b, c$ but $n \neq x$. The r and i indices represent, respectively, the real and imaginary and the components and C_3 and C_4 are presented in (24) and (25).

$$C_3 = \sum_n [(z_{mn_r} - z_{mx_r}) I_{mn_r} - (z_{mn_i} - z_{mx_i}) I_{mn_i}] \tag{24}$$

$$C_4 = \sum_n [(z_{mn_r} - z_{mx_r}) I_{mn_i} + (z_{mn_i} - z_{mx_i}) I_{mn_r}] \tag{25}$$

z_{mn} and z_{mx} indicate the mutual impedance of phases m and x and n, $n \neq x$.

4. Analysis of the results

The analysis of the main results of estimating fault resistance (R_f) and distance (d) in case of faults in unbalanced distribution lines is presented in this section. The tests include several fault scenarios.

4.1. Test network

The test distribution feeder configuration presented in Fig. 3 is based on the IEEE-34-node 301 line, 10 miles long, and operating at 24.9 kV. The per unit line impedance matrix, considering the IEEE 301 feeder, is denoted as z_{301}. This feeder is designed to supply balanced three-phase loads.

$$z_{301} = \begin{bmatrix} 1.930 + j1.412 & 0.233 + j0.644 & 0.236 + j0.569 \\ 0.233 + j0.644 & 1.916 + j1.428 & 0.229 + j0.524 \\ 0.236 + j0.569 & 0.229 + j0.524 & 1.922 + j1.421 \end{bmatrix} \left[\frac{\Omega}{mile}\right]$$

As depicted in Fig. 3, a converter-connected source supplies remote current in the case of single-phase-to-ground (SLG), double-phase (LL), double-phase-to-ground (LLG), and three-phase-to-ground (LLLG) faults along the analysed line and for several fault resistances.

4.2. Analysis of the obtained results

This section presents the absolute error estimation for the fault resistance R_f and distance to the fault d through the proposed algorithm. The absolute error is estimated according to Eq. (26) and (27), and is calculated using the actual or true value (R_f, d) and the estimated value (R_{f_e}, d_e) divided by the total value (R_{f_t}, d_t), which corresponds to the maximum considered fault resistance and the feeder length (50 Ω and 10 miles, respectively).

$$E_{R_f} = 100 \left| \frac{R_f - R_{f_e}}{R_{f_t}} \right| \ [\%] \tag{26}$$

$$E_d = 100 \left| \frac{d - d_e}{d_t} \right| \ [\%] \tag{27}$$

Table 2
Fault resistance estimation error.

Fault	d_f	R_f (Ω)	E_{R_f} (%)	R_f (Ω)	E_{R_f} (%)	R_f (Ω)	E_{R_f} (%)	R_f (Ω)	E_{R_f} (%)
	0		0.0220		0.0298		0.2293		0.5076
	2		0.1180		0.1337		0.2726		0.5800
SLG	4	5	0.1750	10	0.3084	30	0.3090	50	0.6753
	6		0.2207		0.4557		0.4659		0.6949
	8		0.2836		0.5568		0.7710		0.7895
	10		0.3336		0.6448		0.7959		0.8653
	0		0.0047		0.0214		0.2078		0.6599
	2		0.0061		0.0290		0.2173		0.6495
LL	4	5	0.0130	10	0.0298	30	0.2242	50	0.6677
	6		0.0240		0.1049		0.2371		0.6785
	8		0.0345		0.1181		0.2423		0.6871
	10		0.0446		0.1751		0.2558		0.6964
	0		0.0023		0.0204		0.2074		0.6496
	2		0.0024		0.0209		0.2167		0.6590
LLG	4	5	0.0119	10	0.0220	30	0.2277	50	0.6699
	6		0.0227		0.0240		0.2366		0.6709
	8		0.0347		0.1020		0.2439		0.6844
	10		0.0457		0.1070		0.2524		0.6965
	2		0.0009		0.0037		0.2422		0.6412
	2		0.0021		0.0039		0.2440		0.6490
LLLG	4	5	0.0097	10	0.0128	30	0.2564	50	0.6674
	6		0.0187		0.0218		0.2672		0.6734
	8		0.0338		0.1012		0.2719		0.6815
	10		0.0416		0.1810		0.2836		0.6848

4.2.1. Comparative analysis of the distance relay proposal

This section presents a comparative behaviour of the proposed distance relay and the conventional. In this sense, a comparison of the fault distance estimation is given when considering a fault resistance of 5 Ω along the test network. The conventional distance relay is explained in Section 2.1.

Fig. 4 compares the proposed and the conventional relay, considering the distance estimation error (E_d). The results show that the proposed relay surpasses the conventional distance relay as higher errors for the four fault types considered is approximately 0.5% for the single-line-to-ground fault. In contrast, for the conventional relay, errors reach 18.5% for line-to-line fault. The following sections include new and extensive results of the tests performed on the proposed relay.

4.2.2. Results of fault resistance effect

As demonstrated in Table 2, the fault resistance estimation algorithm is feasible since it presents a low and acceptable estimation error for different fault types and various distances.

4.2.3. Results of the fault distance

The proposed method is helpful for distance estimation, as it already determines a fault distance very close to the actual value, as shown in the Table 3.

In all tables, f is the fault type, and d_f is the distance in miles.

4.3. Analysis of results

The proposed algorithm reliably estimates the fault resistance and distance while achieving low estimation errors. Notably, these errors follow a consistent pattern where an increase in fault resistance and distance corresponds to a higher error magnitude. This coherence reinforces the algorithm's potential, as accurate estimations of these parameters will enhance distance relay performance and mitigate the impact of fault resistance, especially in the context of power system fault analysis.

Therefore, the results obtained from this research indicate that this algorithm has proven to be highly efficient and accurate in estimating fault resistance (R_f) and fault distance (d_f). The analysis can be summarised as follows:

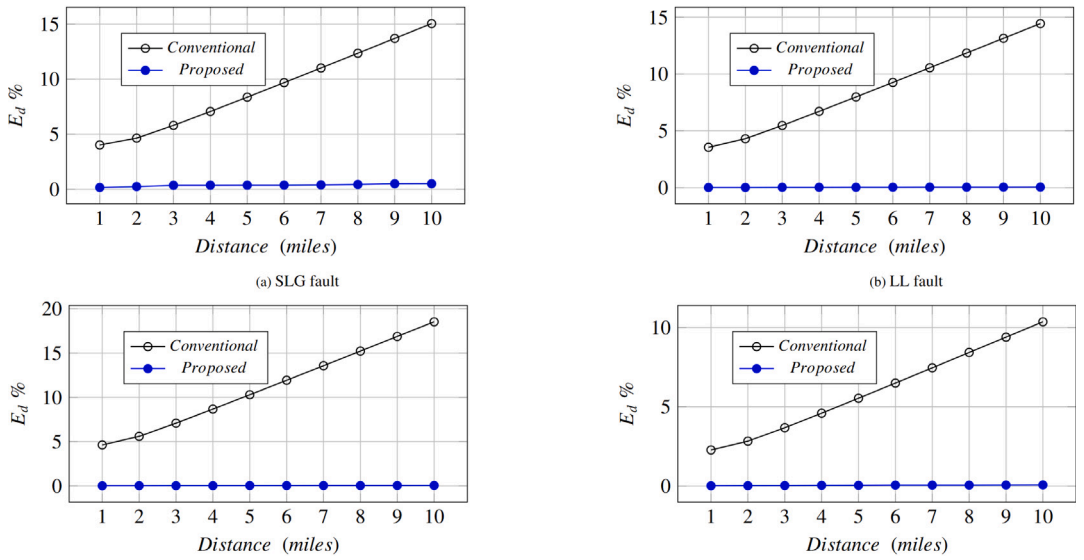

Fig. 4. Fault distance estimation error considering a 10Ω along the IEEE 301 feeder.

Table 3
Fault distance estimation error.

Fault	d_f	R_f (Ω)	E_d (%)	R_f (Ω)	E_d (%)	R_f (Ω)	E_d (%)	R_f (Ω)	E_d (%)
	0		0.0261		0.0831		0.1256		0.3093
	2		0.2408		0.3958		0.3970		0.3983
SLG	4	5	0.3066	10	0.7767	30	0.9666	50	0.9732
	6		0.3720		1.0243		1.0615		1.3809
	8		0.4382		1.1606		1.4770		1.5659
	10		0.5042		1.2957		3.3834		3.4472
	0		0.0229		0.0634		0.4056		1.0354
	2		0.0295		0.0764		0.4457		1.1032
LL	4	5	0.0362	10	0.0895	30	0.4856	50	1.1717
	6		0.0429		0.1031		0.5240		1.2390
	8		0.0497		0.1166		0.5624		1.3065
	10		0.0566		0.1300		0.6004		1.3699
	0		0.0230		0.0636		0.4053		1.0339
	2		0.0353		0.0753		0.4457		1.1005
LLG	4	5	0.0373	10	0.0909	30	0.4855	50	1.1708
	6		0.0436		0.1041		0.5234		1.2386
	8		0.0489		0.1159		0.5597		1.2997
	10		0.0561		0.1298		0.5981		1.3637
	0		0.0232		0.0638		0.4061		1.0360
	2		0.0310		0.0777		0.4457		1.1049
LLLG	4	5	0.0479	10	0.1023	30	0.4963	50	1.1847
	6		0.0624		0.1244		0.5427		1.2564
	8		0.0642		0.1254		0.5664		1.3084
	10		0.0753		0.1518		0.6202		1.3872

- Low estimation errors: The most notable achievement of this algorithm is the consistently low estimation errors. The approach consistently yielded values of less than 1% for R_f and less than 3.5% for d_f. This precision significantly improves over conventional distance protection, which struggles to achieve such low error rates when the fault resistance effect occurs. This level of accuracy is a noteworthy advancement in the field of fault distance estimation.
- Estimation of other variables: Beyond fault resistance and distance, the algorithm's capability to estimate CIDER's fault current and load current ($\boldsymbol{I}_L$) is a significant advance as it provides insight into the state of the network downstream of the fault. This method also accurately estimates fault voltage ($\boldsymbol{U}_f$) and fault current ($\boldsymbol{I}_f$). These estimations are vital for understanding the magnitude of fault conditions and guiding protective actions within the power system. Therefore, this approach provides valuable insights into fault analysis.
- Robustness for all analysed fault types: The algorithm's robustness was particularly evident in its performance across different fault types and distances. It maintained its accuracy and low error rates irrespective of the type of fault under consideration. This adaptability and consistency make it a valuable tool for dealing with various fault scenarios.

Therefore, the obtained results are promising for applying distance relays in unbalanced ADNs. These findings significantly contribute to the protection of such networks, emphasising the algorithm's ability to accurately estimate fault resistance and distance, thereby enhancing the overall performance of relays 21. The successful integration of this algorithm holds promise for effectively protecting unbalanced distribution networks using CIDERs or any other form used to integrate distributed energy resources, marking a notable step towards developing resilient and efficient power systems.

4.4. Computational burden

The computational burden to accurately estimate the fault resistance and distance parameters is minimal. Phasor estimation uses a one-sample recursive FFT algorithm, considering $\frac{1}{4}$ signal cycle-wide window and 16 samples by cycle. The presented low estimation errors are obtained with an average computation time of approximately 13.3 ms after the fault inception, considering the 96 fault situations presented in Table 2. This computation burden does not affect the online relay operation when estimating the fault impedance and generating the corresponding trip signal.

5. Conclusions

In this study, a fault distance estimation algorithm for protection purposes has been developed and evaluated to increase the redundancy of the protection systems for ADN. Based on the results, it is possible to state the following: (i) High accuracy in R_f and d_f estimation is obtained as an error rate below 3.5% in all tested cases. This level of precision makes it a protection tool for ADNs, as it accurately locates faults, regardless of their nature and distance. (ii) The approach's capability to estimate fault current, downstream load current, fault voltage, and fault current provides power system operators with a more comprehensive view of fault conditions. This information enables

quicker fault identification and isolation, improving grid resilience and service reliability. (iii) The method's robust performance across various fault scenarios and distances highlights its adaptability and practicality. It can be applied in diverse operating conditions and proves highly reliable. (iv) The implications of this research extend to real-world ADN, where accurate fault resistance and distance estimation are critical. Implementing this algorithm into practical protection systems can enhance protection redundancy and grid reliability, reduce downtime, and improve the quality of electric service.

Finally, the proposed fault resistance and distance estimation algorithm demonstrates exceptional accuracy and adaptability, making it essential to unbalanced ADN protection systems and fault analysis. Its potential impact on the reliability and resilience of unbalanced power distribution networks is significant, and future work should focus on its practical implementation and further refinement.

CRediT authorship contribution statement

S. Velasco-Gómez: Writing – original draft, Validation, Methodology, Investigation, Formal analysis. **S. Pérez-Londoño:** Writing – review & editing, Validation, Methodology, Formal analysis. **J. Mora-Flórez:** Supervision, Methodology, Funding acquisition, Conceptualization.

Declaration of competing interest

The authors declare the following financial interests/personal relationships which may be considered as potential competing interests: J. Mora-Florez reports financial support was provided by Minciencias Colombia and Technological University of Pereira.

Acknowledgements

This research outcome received funding from Minciencias - Colombia (INTEGRA2023 - 80740-774-2020) and the Universidad Tecnológica de Pereira. The ICE^3 research group contributed to the development of this product.

Data availability

Data will be made available on request.

References

Abdollahzadeh, Hamed, 2023. A distance protection/fault location algorithm for double-circuit transmission lines with asymmetrical circuits during cross-country faults. Int. J. Electr. Power Energy Syst. 148, 108943.

Assouak, Asma, Benabid, Rabah, 2023. A new coordination scheme of directional overcurrent and distance protection relays considering time-voltage-current characteristics. Int. J. Electr. Power Energy Syst. 150, 109091.

Bahrani, Behrooz, 2021. Power-synchronized grid-following inverter without a phase-locked loop. IEEE Access 9, 112163–112176.

Banaiemoqadam, Amin, Hooshyar, Ali, Azzouz, Maher A., 2020. A control-based solution for distance protection of lines connected to converter-interfaced sources during asymmetrical faults. IEEE Trans. Power Deliv. 35 (3), 1455–1466.

Biller, Martin, Jaeger, Johann, 2022. Protection algorithms for closed-ring grids with distributed generation. IEEE Trans. Power Deliv. 37 (5), 4042–4052.

Chao, Chenxu, Zheng, Xiaodong, Weng, Yang, Liu, Yu, Gao, Piao, Tai, Nengling, 2022. Adaptive distance protection based on the analytical model of additional impedance for inverter-interfaced renewable power plants during asymmetrical faults. IEEE Trans. Power Deliv. 37 (5), 3823–3834.

Filomena, André Darós, Salim, Rodrigo Hartstein, Resener, Mariana, Bretas, Arturo Suman, 2008. Ground distance relaying with fault-resistance compensation for unbalanced systems. IEEE Trans. Power Deliv. 23 (3), 1319–1326.

García-Ceballos, C., Pérez-Londoño, S., Mora-Flórez, J., 2021. Integration of distributed energy resource models in the VSC control for microgrid applications. Electr. Power Syst. Res. 196, 107278.

García-Ceballos, C., Pérez-Londoño, S., Mora-Flórez, J., 2023. Stability analysis framework for isolated microgrids with energy resources integrated using voltage source converters. Results Eng. 19, 101252.

George, Neethu, Naidu, O.D., Pradhan, Ashok Kumar, 2023. Distance protection for lines connecting converter interfaced renewable power plants: Adaptive to grid-end structural changes. IEEE Trans. Power Deliv. 38 (3), 2011–2021.

Ghorbani, Amir, Mehrjerdi, Hasan, 2023. Distance protection with fault resistance compensation for lines connected to PV plant. Int. J. Electr. Power Energy Syst. 148, 108976.

Gutierrez-Rojas, Daniel, Nardelli, Pedro Henrique Juliano, Mendes, Goncalo, Popovski, Petar, 2020. Review of the state of the art on adaptive protection for microgrids based on communications. IEEE Trans. Ind. Inform. 17 (3), 1539–1552.

Hooshyar, Ali, Azzouz, Maher A., El-Saadany, Ehab F., 2014. Distance protection of lines emanating from full-scale converter-interfaced renewable energy power plants—Part I: Problem statement. IEEE Trans. Power Deliv. 30 (4), 1770–1780.

Hooshyar, Ali, Iravani, Reza, 2017. Microgrid protection. Proc. IEEE 105 (7), 1332–1353.

Li, Bin, Sheng, Yaru, He, Jiawei, Li, Ye, Xie, Zhongrun, Cao, Yunzhu, 2023. Improved distance protection for wind farm transmission line based on dynamic frequency estimation. Int. J. Electr. Power Energy Syst. 153, 109382.

Liang, Yingyu, Li, Wulin, Lu, Zhengjie, Xu, Guanjun, Wang, Cong, 2020. A new distance protection scheme based on improved virtual measured voltage. IEEE Trans. Power Deliv. 35 (2), 774–786.

Mishra, Priyanka, Pradhan, Ashok Kumar, Bajpai, Prabodh, 2020. Adaptive distance relaying for distribution lines connecting inverter-interfaced solar PV plant. IEEE Trans. Ind. Electron. 68 (3), 2300–2309.

Mishra, Priyanka, Pradhan, Ashok Kumar, Bajpai, Prabodh, 2021. Adaptive distance relaying for distribution lines connecting inverter-interfaced solar PV plant. IEEE Trans. Ind. Electron. 68 (3), 2300–2309.

Song, Guobing, Chang, Peng, Hou, Junjie, Li, Weijia, Zhang, Chenhao, 2023. A time-domain distance protection method applicable to inverter-interfaced systems. Electr. Power Syst. Res. 225, 109806.

Tang, Liangyu, Han, Yang, Zalhaf, Amr S., Zhou, Siyu, Yang, Ping, Wang, Congling, Huang, Tao, 2024. Resilience enhancement of active distribution networks under extreme disaster scenarios: A comprehensive overview of fault location strategies. Renew. Sustain. Energy Rev. 189, 113898.

Tsimtsios, Aristotelis M., Korres, George N., Nikolaidis, Vassilis C., 2019a. A pilot-based distance protection scheme for meshed distribution systems with distributed generation. Int. J. Electr. Power Energy Syst. 105, 454–469.

Tsimtsios, Aristotelis M., Safigianni, Anastasia S., Nikolaidis, Vassilis C., 2019b. Generalized distance-based protection design for dg integrated mv radial distribution networks—part i: Guidelines. Electr. Power Syst. Res. 176, 105949.

Uzair, Muhammad, Li, Li, Eskandari, Mohsen, Hossain, Jahangir, Zhu, Jian Guo, 2023. Challenges, advances and future trends in AC microgrid protection: With a focus on intelligent learning methods. Renew. Sustain. Energy Rev. 178, 113228.

Uzair, Muhammad, Li, Li, Zhu, Jian Guo, Eskandari, Mohsen, 2019. A protection scheme for AC microgrids based on multi-agent system combined with machine learning. In: 2019 29th Australasian Universities Power Engineering Conference. AUPEC, pp. 1–6.

Velasco-Gómez, Sara María, Pérez-Londoño, Sandra Milena, Mora-Flórez, Juan José, 2021. A qualitative comparison of distance-based protection approaches for active distribution networks. Tecnura 25 (70), 147–165.

Velasco-Gómez, S., Pérez-Londoño, S., Mora-Floréz, J., 2023. Unbalance compensated distance relay for active distribution networks. Energy Rep. 9, 438–446.

Yin, Yujie, Fu, Yong, Zhang, Zhiying, Zamani, Amin, 2022. Protection of microgrid interconnection lines using distance relay with residual voltage compensations. IEEE Trans. Power Deliv. 37 (1), 486–495.

Zhang, Xiaoyou, Radwan, Mohamed, Azad, Sahar Pirooz, 2023. Modified distance protection of transmission lines originating from DFIG-based WPPs by considering the impact of fault-induced rotor frequency and LVRT requirements. Int. J. Electr. Power Energy Syst. 147, 108911.

Zhang, Haobo, Xiang, Wang, Hong, Qiteng, Wen, Jinyu, 2022. Active phase control to enhance distance relay in converter-interfaced renewable energy systems. Int. J. Electr. Power Energy Syst. 143, 108433.